W-87

ACR No. 4J28

NATIONAL ADVISORY COMMITTEE FOR AERONAUTICS

WARTIME REPORT

ORIGINALLY ISSUED

February 1945 as
Advance Confidential Report 4J28

INVESTIGATION OF BOUNDARY LAYER TRANSITION ON CONCAVE WALLS

By H. W. Liepmann
California Institute of Technology

NACA

WASHINGTON

NACA ACR No. 4J28

NATIONAL ADVISORY COMMITTEE FOR AERONAUTICS

ADVANCE CONFIDENTIAL REPORT

INVESTIGATION OF BOUNDARY LAYER TRANSITION ON CONCAVE WALLS

By H. W. Liepmann

SUMMARY

Transition of the boundary layer from the laminar to the turbulent regime was investigated on the concave side of a plate with a radius of curvature of 2.5 feet. The critical Reynolds number was found to be considerably lower than on a flat plate and on the concave side of a plate with a 20-foot radius of curvature previously investigated. It was furthermore found that, in agreement with the theoretical results of Görtler, $R_\theta\sqrt{\frac{\theta}{r}}$, here termed the "Görtler parameter," is the proper critical parameter governing boundary layer instability due to concave curvature. The critical parameter at transition was found to have a value of 9.0.

The influence of pressure gradient and of an increased free-stream turbulence level on the position of the transition point on the concave side of the plate of 2.5-foot radius of curvature has been studied. Small variations of the pressure gradient did not alter the value of the critical Görtler parameter. This result is compared with similar measurements on the convex side of a plate of 20-foot radius of curvature. Increased tunnel turbulence lowered the value of the critical parameter 9.0 at a turbulence level of 0.06 percent to 6.0 at a turbulence level of 0.3 percent.

The investigation confirms the previous result that the mechanism of the breakdown of the laminar boundary layer is essentially different on convex and concave boundaries.

A discussion of the practical applicability of transition measurements is given, and the difference betweeen critical Reynolds number corresponding to laminar instability and critical Reynolds number corresponding to transition is pointed

out. A definition of transition Reynolds number, based on the apparent shearing stress caused by the laminar oscillations, is given. In the case of flow along a flat plate, values of transition Reynolds number are calculated approximately for different intensities of the initial disturbance.

INTRODUCTION

The larger part of the California Institute of Technology investigation on the effect of curvature on boundary layer stability and transition has been previously reported (reference 1). This previous research led to the conclusion that the mechanism of the breakdown of the laminar boundary layer is essentially different on concave and convex walls. The instability of the laminar boundary layer on convex boundaries was found to be brought about by plane disturbances, the so-called Tollmien-Schlichting waves, which were first observed by Dryden, Schubauer, and Skramstad on a flat plate. The range of unstable frequencies and the amplification characteristics of the Tollmien-Schlichting waves were found, within the experimental scatter, to be the same on the convexly curved boundaries as had earlier been observed by Schubauer and Skramstad (reference 2) on the flat plate. It was accordingly concluded that the transition point was essentially unaffected by convex curvature. These measurements extended over a range of effective curvature θ/r from 0 to 10^{-3}, where θ is the momentum thickness of the boundary layer and r is the radius of curvature of the boundary.

Concave curvature was found to have a pronounced destabilizing effect on the laminar boundary layer, the critical Reynolds number decreasing with increasing effective curvature. It was, therefore, concluded that the mechanism of transition on concave walls was different from that on flat and convex boundaries. It was furthermore shown that these observations were in general agreement with theoretical results of Görtler (reference 3) which predicted a strong dynamic instability due to three-dimensional disturbances on concave boundaries. The measurements for the case of concave boundaries were, however, not so extensive as for the convex case and covered only the range of effective curvature between 0 and 0.0001. One purpose of the investigations reported here is the extension of the previous measurements to values of effective curvature of about 0.001 on a concave boundary.

The influence of the pressure gradient along the laminar boundary layer on the position of the transition point has long

been known. The measurements which have been carried out before were always confined to flat-plate flow or flow past convex boundaries. Based on Görtler's theoretical results it was suggested in the previous report that the influence of pressure gradient on transition should be less pronounced on concave boundaries. Consequently, measurements of the effect of pressure gradient on the position of the transition point have been carried out and the results are presented in the present report. The effect of an increased free-stream turbulence level on transition was also studied.

The investigations reported here confirm and supplement the results reported previously, and thus conclude the research program on the influence of curvature on boundary-layer transition carried out over a number of years at the California Institute of Technology under the sponsorship and with the financial assistance of the National Advisory Committee for Aeronautics.

The continuous interest, encouragement, and advice of Dr. Th. von Kármán and Dr. C. B. Millikan is gratefully acknowledged. The author also wishes to acknowledge many helpful discussions with Dr. C. C. Lin, and the assistance of Mr. J. Laufer.

SYMBOLS

x	distance along surface of plate from leading edge
y	distance perpendicular from surface
z	distance along surface perpendicular from leading edge
r	radius of curvature of the boundary layer
U	mean velocity at a point in the boundary layer
U_o	mean velocity of the free stream
u	instantaneous x-component of fluctuation velocity
v	instantaneous y-component of fluctuation velocity
w	instantaneous z-component of fluctuation velocity

u', v', w' root-mean-square values of u, v, and w, respectively

$\frac{u'}{U_o}$ etc., turbulence level, usually expressed in percent

ρ density

μ viscosity

$\nu = \frac{\mu}{\rho}$ kinematic viscosity

$q = \frac{1}{2}\rho U_o^2$ dynamic pressure of the free stream

$\eta = y\sqrt{\frac{U_o}{\nu x}}$ Blasius' nondimensional parameter

δ boundary layer thickness

δ^* boundary layer displacement thickness

θ boundary layer momentum thickness

$\frac{\theta}{r}$ effective curvature of the boundary layer

R Reynolds number

R_x, R_θ, R_{δ^*} Reynolds numbers based on x, θ, and δ^*, respectively, $R_x = U_{ox}/\nu$ = x-Reynolds number, and so forth

$R_{x_{tr}}$, $R_{\theta_{tr}}$, $R_{\delta^*_{tr}}$ Reynolds numbers at the transition point

$R_\theta\sqrt{\frac{\theta}{r}}$ Görtler parameter

$\tau_A = -\rho\,\overline{uv}$ apparent shear

$\tau_L = \mu\frac{du}{dy}$ laminar shear

$k = \frac{\overline{uv}}{u'v'}$ correlation coefficient

c_{f_L} laminar skin-friction coefficient

APPARATUS AND METHODS

Wind Tunnel and Test Section

The general layout of the wind tunnel is shown in figure 1. A detailed description can be found in reference 1. The measurements were carried out on the concave side of a smooth glass plate of 2.5-foot radius of curvature. This plate was set in the center of the high (5 ft) and narrow (7.5 in.) test section shown in figure 2. The section consists essentially of two plate-glass plates forming cylinders concentric with the center sheet, on which the measurements are made. These plates are mounted in wooden frames which, by means of a screw adjustment, allow a variation of the width of the channel and of the angle of attack of the center plate. This adjustment makes it possible to alter the pressure gradient along the test section. Owing to the geometry of the section it is, however, difficult to set for a predetermined simple pressure distribution, for example, a linear distribution. The investigations on the effect of pressure gradient on transition were, therefore, rather tedious and the investigated range of pressure gradients limited.

Free-Stream Turbulence Level

The normal free-stream turbulence level of the tunnel was the same as in the previous measurements. The values were

$$\frac{u'}{U_o} = 0.06 \text{ percent}$$

$$\frac{v'}{U_o} = \frac{w'}{U_o} = 0.12 \text{ percent}$$

The turbulence level in the test section is mainly controlled by the precision screen "S" (fig. 1) in the pressure chamber. To investigate the position of the transition point at higher

turbulence levels of the free stream, the tunnel turbulence was artificially raised in the following way: Strips of celluloid tape about 1 inch wide and 5 inches long were glued at regular intervals of about 3 inches on the downstream side of the screen S. These strips produced a uniform turbulence level of

$$\frac{u'}{U_o} = 0.3 \text{ percent}$$

in the test section. By removing every second strip, and so forth, the turbulence level could then be lowered to the normal free stream level.

Traversing Mechanism

The traversing mechanism used in this wind tunnel is described in detail in reference 1. The motion of the instrument, for example, hot-wire anemometer, is continuous in the x and y directions and is remotely controlled.

Hot-Wire Anemometer

The mean-speed distribution in the boundary layer was measured with platinum wires of 0.0005-inch diameter and about 5-millimeter length. The turbulence level and the position of the transition point were determined with 0.00024-inch thick and about 2-millimeter long wires. Mean speed was always measured using the constant-resistance method. For measurements of velocity fluctuations the wire was calibrated using the electrical oscillator method (reference 4) and the amplifier properly compensated by means of an inductance-resistance circuit. The amplifier response is flat between less than 5 cycles up to 8000 cycles.

Measurement of the Pressure Distribution

The pressure distribution along the test section was measured by means of a small static tube mounted on the instrument carriage at a distance of about 1 centimeter from the test plate. Thus, the pressure gradient close to the edge of the boundary layer was measured. The irregular "waves" in the distribution (fig. 3) are due to local changes in the radius of curvature of the plate.

Determination of the Transition Point

The transition point was determined by means of the hot-wire anemometer. The hot wire was mounted on the instrument carriage a few thousandths of an inch from the surface of the plate. The carriage was then moved slowly in the direction of the mean flow from the leading edge downstream; the first appearance of the turbulent bursts (see reference 1) on the oscilloscope screen was taken as indication of transition.

MEASUREMENTS AND RESULTS

Mean Speed Distribution

The test-section walls were adjusted to give a pressure gradient as close to zero as possible. The best result which could be obtained is shown as "A" in figure 3. The pressure gradient is seen to be close to zero over the first 90 centimeters of the test plate. Since transition was found to occur at distances from the leading edge of less than 60 centimeters, this pressure gradient A (fig. 3) could, with sufficient approximation, be taken as "zero" gradient. The velocity distribution in the laminar boundary layer was then measured. The result is shown in figure 4. It is seen, that the profile follows, rather closely, the Blasius flat-plate profile. There exists a slight systematic deviation from the Blasius profile especially in the range between $\eta = 3$ and $\eta = 6$. The measured values of $\frac{u}{U_o}$ are slightly lower than the ones given by the Blasius distribution.

The main purpose of the measurements was to establish whether computations of the momentum thickness θ, the Reynolds number based on θ, and so forth could be computed from the Blasius solution. For computation of these data applied to transition measurements, the slight deviation seen in figure 4 is immaterial and consequently the values of θ, δ^*, and so forth, used later on, have been computed from the Blasius formula, that is,

$$\theta = \frac{2}{3}\sqrt{\frac{\nu x}{U_o}}$$

$$\delta^* = 1.73\sqrt{\frac{\nu x}{U_o}}$$

Effect of Curvature on the Position of the Transition Point

Transition was measured with the hot-wire anemometer. By varying the velocity of the free stream, the range of effective curvature from -0.5×10^{-4} to -1.1×10^{-4} could be investigated. The results of the tests are shown in figure 5 where the critical Reynolds number $R_{x\,tr}$ is plotted versus $\frac{\theta}{r}$. It is seen that $R_{x\,tr}$ falls from about 4×10^5 at $\frac{\theta}{r} = -5 \times 10^{-4}$ to 1.5×10^5 at $\frac{\theta}{r} = -11 \times 10^{-4}$. This result agrees very well with previous measurements (reference 1). Figure 6 shows the effect of curvature on transition for effective curvature ranging from -0.001 (concave)) to $+0.001$ (convex). Here $R_{\theta\,tr}$ is plotted versus $\frac{\theta}{r}$. It is seen that the decrease of the critical number found on the concave side of the 20-foot plate continues with higher effective curvature.

According to Görtler (reference 3) $R_\theta \sqrt{\frac{\theta}{r}}$ is the characteristic parameter for the three-dimensional instability on concave walls. If the value of this parameter at transition is plotted versus effective curvature (fig. 7a), it is seen that within the rather large scatter the value of $\left(R_\theta \sqrt{\frac{\theta}{r}}\right)_{tr}$ does not systematically vary with $\frac{\theta}{r}$. The average value of $\left(R_\theta \sqrt{\frac{\theta}{r}}\right)_{tr}$ found is about 9.0. The value of the parameter as measured here is somewhat larger than the value of 7.3 found previously on the concave side of the plate of 20-foot radius. There exists a possible explanation for this difference in the value of the Görtler parameter at transition which can best be seen from a plot such as figure 8.

Instead of plotting the Görtler parameter as a function of effective curvature $R_{x\,tr}$ is plotted as a function of $\frac{r}{\theta}$. Since $R_x \approx R_\theta^2$, $R_\theta \sqrt{\frac{\theta}{r}} = \text{constant}$ corresponds to straight lines through the origin in this plot. The measured values of $R_{x\,tr}$ for the two test sections of 20-foot and 2.5-foot radius are presented in figure 8, and in addition, the line $R_\theta = 9.4 \times 10^2$ corresponding to transition on a

flat plate in the wind tunnel is shown. Assume that transition due to Görtler vortices occurs for all concave curvatures at the value of $R_\theta \sqrt{\frac{\theta}{r}}$ found on the plate of 2.5-foot radius. All transition measurements should thus fall on the straight line $\left(R_\theta \sqrt{\frac{\theta}{r}}\right)_{tr} = 9.0$ (fig. 8). Transition on the flat plate, that is, transition caused by the two-dimensional perturbation, was found to occur at $R_{\theta tr} = 9.4 \times 10^{-2}$. Since the Tollmien-Schlichting wave is but little affected by small curvature, it can be expected that transition caused by this disturbance on slightly concave plates occurs at about the same R_θ. Hence, starting from the flat plate, all transition measurements should follow the straight line $R_\theta = 9.4 \times 10^{2}$ in figure 8. At $\frac{r}{\theta} = -11 \times 10^{3}$ the line $\left(R_\theta \sqrt{\frac{\theta}{r}}\right)_{tr} = 9.0$ and $R_\theta = 9.4 \times 10^{-2}$ intersect; that is, at effective curvatures larger than -11×10^{3} transition is caused by the three-dimensional disturbance. At smaller effective curvature the Tollmien-Schlichting wave is more unstable and thus is responsible for transition. It appears that this is not the case, but that a more or less continuous change from the transition due to Görtler vortices to transition caused by Tollmien-Schlichting waves takes place. Since the laminar boundary layer on concave walls is unstable with respect to small perturbations of both kinds, such a continuous change is possible and probable. Both types of perturbation are excited by the external free-stream turbulence, traveling downstream, that is, toward higher values of R_δ both the waves or the vortices of a given wavelength increase in amplitude when they pass through their respective instability region in the $R_{\delta^*}-\alpha$ diagram (see reference 1). A transfer of energy from the one type of perturbation to the other is therefore quite possible and such a transfer becomes unimportant only if one of these perturbations is considerably more unstable than the other, that is, in the limiting cases of small and large effective curvature. A more exact analysis of such an energy transfer is impossible without a detailed knowledge of the amplification of both types of perturbation and furthermore of the excitation due to free stream turbulence.

Effect of the Pressure Gradient on Transition

It is well known that a pressure gradient along a laminar boundary layer strongly influences the position of the transition point. The so-called low-drag or laminar flow airfoil represents an application of this result. All investigations on the influence of the pressure gradient have previously, however, been confined to measurements on flat or convexly curved boundaries, that is, to boundary layer flows, where the Tollmien-Schlichting instability is predominant. Based on the theoretical analysis of Görtler (reference 3) it was suggested previously (reference 1) that the influence of the pressure gradient on transition should be less pronounced on concave walls where the boundary-layer instability should be due to the three-dimensional vortices.

To investigate this question, measurements of the influence of pressure gradient on transition were carried out on the convex side of the plate of 20-foot radius and on the concave side of the plate of 2.5-foot radius. Thus, a typical Tollmien-Schlichting and Görtler case could be compared. The pressure distributions for which transition was investigated are shown in figures 3 and 9, respectively. Before a discussion and comparison of the measurements can be presented, the question of the proper parameter for the pressure gradient and the proper critical number for transition must be discussed.

It is sometimes useful to present transition data in the form of a critical Reynolds number R_x based on the distance from the leading edge, that is, from the stagnation point. However, R_x certainly is not the proper physical parameter, and it is preferable to base the critical number on some measure of the local boundary layer thickness. The momentum thickness appears as the best choice since it is closely connected with the shearing stress at the wall and thus with the slope of the velocity profile at the wall. In this connection the instability of a velocity profile with respect to Tollmien-Schlichting waves is known to depend very much on the slope (and curvature) of the profile in the neighborhood of the wall. Görtler found that for the three-dimensional disturbance also momentum thickness is the most suitable length for the critical parameter. Thus it appears reasonable to plot for flat and convex surfaces the critical number $R_{\theta_{tr}}$ and for the concave surfaces $\left(R_\theta \sqrt{\frac{\theta}{r}}\right)_{tr}$ as functions of some effective pressure gradient. To represent the pressure gradient, that is, $\frac{1}{q}\frac{dp}{dx}$ in dimensionless form, a length is again needed.

The effective force acting on an element of the boundary layer is the force due to the pressure gradient, $\frac{\delta}{q}\frac{dp}{dx}$. The boundary layer thickness δ entering here has more kinematic than dynamic character and thus the displacement thickness δ^* appears as the logical choice. This can also be seen from von Kármán's momentum equation of the boundary layer

$$\frac{\tau_o}{q} = \frac{1}{q}\frac{d(\theta q)}{dx} - \frac{\delta^*}{q}\frac{dp}{dx}$$

where also the combination $\frac{\delta^*}{q}\frac{dp}{dx}$ appears.

The results of the measurements are, therefore, represented in the form $R_{\theta_{tr}}$ and $\left(R_\theta\sqrt{\frac{\theta}{r}}\right)_{tr}$, respectively, versus $\frac{\delta^*}{q}\frac{dp}{dx}$. It is, of course, not to be expected that a complicated phenomenon, such as the laminar instability for flow with pressure gradient, can be described by one critical parameter alone. Under the influence of the pressure gradient, the velocity profile of the layer will, in fact, change continuously from the stagnation point up to eventual separation. The instability zones for small perturbations and the amplification characteristics thus vary continuously downstream. Transition occurs if perturbations are amplified to a sufficient degree. Since the total amplification is thus an integral effect depending on all instability zones passed by the perturbation on the way from its origin downstream to the transition point, it seems hardly possible to give a representation involving only one critical number such as R_θ. Only where the instability zones are little affected by a change in the profile as, for example, according to Görtler (reference 3), in the case of flow past concave boundaries can it be expected that it will be possible to represent the instability character by only one critical parameter, in this case $R_\theta\sqrt{\frac{\theta}{r}}$. Except for pressure gradient "C" on the convex side of the plate of 20-foot radius, the momentum thickness and displacement thickness were again computed using the Blasius solution. The influence of these comparatively small gradients on the boundary-layer thickness was found to be negligible within the scatter of the transition measurements. In the case of gradient C in figure 9, the momentum thickness and displacement thickness were computed from the solution of the laminar boundary-layer equations for the case of a linear decrease of the free-stream velocity. The experimentally determined

pressure distribution was approximated by a parabola, and the momentum and displacement thicknesses were determined from the tabulated solution (reference 5). It is seen from figure 10 that for the case of convex curvature $R_{\theta_{tr}}$ decreases with positive and increases with negative pressure gradient as expected. The largest decrease with positive pressure gradients occurs close to zero pressure gradient. Whether or not this is true for negative gradients remains undecided since no measurements at larger negative values of $\frac{\delta^*}{q}\frac{dp}{dx}$ could be carried out due to the limited Reynolds number of the test plates. The rapid change of $R_{\theta_{tr}}$ in the neighborhood of zero pressure gradient and the comparatively small change at larger positive values of $\frac{\delta^*}{q}\frac{dp}{dx}$ is interesting. Thus it is indicated that the Blasius solution is singular in the sense that a slight variation of the profile from the Blasius solution does cause large changes in the stability character. This is not unreasonable since the Blasius solution is indeed a singular solution with $\frac{\partial^2 u}{\partial y^2} = 0$ at $y = 0$. A theoretical analysis of the instability character of profiles where the pressure gradient is not zero but is small will be required for a physical explanation of this pressure-gradient effect.

The absolute values given in figure 10 for $R_{\theta_{tr}}$ as a function of $\frac{\delta^*}{q}\frac{dp}{dx}$ are certainly not universally applicable since they are strongly influenced by the wind-tunnel characteristics, that is, turbulence level, turbulence spectrum, and so forth (see also reference 1). The relative variation of the critical Reynolds number at transition with pressure gradient, however, is believed to be quite general. Consequently, it is to be expected that in practical applications, such as the laminar flow wing, and so forth, the movement of the transition point when the pressure gradient is altered is most pronounced in the neighborhood of zero gradient.

Figure 11 shows the effect of pressure gradient on transition on the concave side of the plate of 2.5-foot radius. It is seen that the critical parameter for transition of the boundary layer decreases with increasing pressure gradient. This effect hardly exceeds the scatter of the points, however, and is not believed to be actually systematic. A comparison of the values of the critical parameter for transition at positive gradients with the range

of values at zero pressure gradient shows that the apparent decrease at positive pressure gradient lies within the experimental error. The comparatively large scatter of the points is due to the inherent difficulty of transition measurements on a plate with a small radius of curvature and also to errors in the determination of the boundary layer thickness which enters both parameters $R_\theta \sqrt{\frac{\theta}{r}}$ and $\frac{\delta^*}{q}\frac{dp}{dx}$. The measurements were taken at small values of R_x because of early transition, and thus θ and δ^* vary comparatively rapidly with x. An error in x_{tr} thus produces larger errors in θ_{tr} and δ^*_{tr} than appears in the case of the convex plate where $R_{x_{tr}}$ was five to ten times larger. The present investigation accordingly indicates that the influence of pressure gradient on transition at concave surfaces is either zero or at most very small.

Effect of Free Stream Turbulence on Transition

That free-stream turbulence has a strong influence on the position of the transition point is well established. The first systematic investigation of this effect was made by Schubauer and Skramstad (reference 2), who measured the effect of varied free stream turbulence level on transition of the boundary layer on a flat plate.

In the present investigation, transition was measured on the concave side of the plate of 2.5-foot radius for three turbulence levels of the free stream. The results are given in figure 7. It is seen that an increased turbulence level leads to earlier transition. The critical number $\left(R_\theta \sqrt{\frac{\theta}{r}}\right)_{tr}$ decreases from 9.0 with $\frac{u'}{U_o}$ = 0.06 percent to 6.0 with $\frac{u'}{U_o}$ = 0.3 percent. The magnitude of the turbulence effect is of the same order as in the case of a flat plate (reference 2). Thus it appears that the three-dimensional disturbances, like the Tollmien-Schlichting waves, are excited by turbulence in the free stream. A more detailed discussion of the turbulence effect meets, as in the case of the Tollmien-Schlichting waves, with the difficulty that the phenomenon depends on the spectrum (or on the scale) of tunnel turbulence, and furthermore on the amplification characteristics of the perturbation along the path traveled by the perturbation.

LAMINAR INSTABILITY AND TRANSITION

The preservation of laminar flow up to very large Reynolds numbers is of considerable practical interest. Experimental investigations of transition from the laminar to the turbulent regime have, therefore, been undertaken with a double purpose: To give an understanding of the mechanism of transition or at least of the breakdown of laminar motion, and to permit prediction of the occurrence of transition for a given practical case such as a certain airfoil. The first part of this problem has found a complete solution: Recent experiments (reference 1 and especially reference 2) confirmed, in general, the results of earlier theoretical investigations of Heisenberg, Tollmien, Schlichting, Görtler, and others. On the basis of this experimental and theoretical evidence, and also of earlier work of Taylor on the flow between rotating cylinders, there appears to be no doubt that laminar flow always becomes unstable for a sufficiently large Reynolds number. This critical Reynolds number will depend on the form of the laminar motion, for example, laminar boundary-layer flow, laminar pipe flow, and so forth, and on the type of disturbance, for example, two-dimensional waves or three-dimensional vortices. Instability in the sense used here means that for all Reynolds numbers above the critical one there will exist a range of, say, wavelengths or frequencies such that a disturbance of the proper frequency or wavelength will increase in amplitude.

Thus the mechanism of laminar instability is clear and the critical Reynolds number thus defined can be predicted. However, for practical purposes, it is desirable to predict a different Reynolds number; namely, the Reynolds number at which the flow becomes turbulent. There is a distinct difference between these two Reynolds numbers; if the first Reynolds number R_1, that is, the critical number in the sense of the small perturbation theory, is reached, amplification of certain disturbances begins. The second, or "practical" critical Reynolds number R_2 means that amplification of disturbances has already taken place and to such an extent that complete breakdown of the laminar motion occurs.

The critical Reynolds number R_1 is, in general, so low and the difference between R_1 and R_2 so large that for practical applications the prediction of R_1 only is of little use. For example, the laminar boundary layer along a flat plate in the absence of a pressure gradient becomes theoretically unstable at a Reynolds number based on the

distance from the leading edge, $R_{x_1} = 6 \times 10^4$. Experiments in low-turbulence tunnels (references 1 and 2) confirmed this number but showed also that actual transition occurred only at Reynolds numbers from 2×10^6 to 2.8×10^6. Hence, the larger part of the boundary layer is in most practical cases in an unstable state, that is, in a condition similar to that of a supercooled liquid or a supersaturated vapor. The Reynolds number R_1 corresponds in this analogy to the melting or condensation temperature T_1. The Reynolds number R_2 corresponds to the temperature T_2 at which under given experimental conditions the substance actually solidifies or condenses. Consequently R_1 is a definite number for a certain type of laminar motion, corresponding to the definite melting temperature of a certain substance. On the other hand, R_2 depends not only upon the type of laminar motion but also upon the intial disturbances present in the laminar layer and therefore on the experimental setup, for example, the free stream turbulence level. The amplification of these initial disturbances in the unstable region can be computed from the small perturbation analysis, provided the magnitude of these disturbances does not exceed the range of this linearized theory. Let $a(R_x)$ denote the ratio of the amplitude of a given oscillation at a Reynolds number R_x to that of the same oscillation just upstream of the instability zone. The value $a(R_x)$ depends, of course, on the frequency of the oscillation (see, for example, references 1 and 2). It is now possible to compare $a(R_x)$ for various frequencies and obtain the maximum possible amplification $a(R_x)_{max}$ at a given Reynolds number R_x. Such a computation was carried out by Schlichting (reference 1) for flat-plate flow. Schlichting found in this case

$$a(R_x)_{max} = 0.55\, e^{0.555 \times 10^{-5} R_x} \qquad (1)$$

Comparing his result with measurements of Hansen and Gebers, Schlichting noted that at transition the "most dangerous" frequencies had been amplified four to nine times. However, if the values of R_x found in recent experimental work are inserted into equation (1), $a(R_x)$ becomes of the order of 10^5. This point was emphasized by G. I. Taylor in 1938 (reference 8) and at that time was considered as strong evidence against the validity of the small-perturbation theory. This apparent difficulty in applying equation (1) is mainly caused by the lack of a clear definition of R_2, the Reynolds number of transition; thus, in order to bridge the gap between R_1 and R_2 it is first necessary to define R_2 in such a way that it can be related to the small perturbation theory and hence to R_1.

The following definition appears to be reasonable: "R_2 is the Reynolds number at which the apparent shear $\tau_A = -\rho\,\overline{uv}$ due to amplified boundary layer oscillations at any point in the boundary layer becomes equal to the laminar shear $\tau_L = \mu \frac{du}{dy}$ in the boundary layer." Beginning with R_1, certain disturbances will be amplified. The perturbation components u and v are correlated and consequently give rise to an apparent shear. The magnitude of this apparent shear increases as the amplitude of the oscillations increases. When this apparent shear becomes of the same order as the laminar shear of the undisturbed mean motion the mean profile can evidently no longer remain unaltered. Hence, R_2 defined in this way can be expected to be reasonably close to the Reynolds number at which the oscillation has an effect on the mean flow sufficient to modify radically the mean velocity profile.

The shear which exists in the undisturbed laminar motion τ_L can be computed as a function of R_x for any given case. The apparent shear caused by amplified boundary layer oscillations τ_A, is more difficult to compute since τ_A depends upon the initial disturbance in the laminar layer and the amplification characteristics.

It is, however, possible to bring τ_A into a form where its general behavior as a function of R_x becomes more evident and where in certain cases, at least the order of magnitude of τ_A and thus of R_2 can be obtained by crude approximations.

If the correlation coefficient $k = \frac{\overline{u\,v}}{u'v'}$ and the fluctuation levels $\frac{u'}{U_o}$ and $\frac{v'}{U_o}$ are introduced, τ_A becomes

$$\tau_A = -\rho\,\overline{uv} = -\rho\,k\,\frac{u'}{U_o}\,\frac{v'}{U_o}\,U_o^2$$

It is furthermore convenient to introduce a factor b by writing

$$b\,\frac{u'}{U_o} = \frac{v'}{U_o}$$

and thus

$$\frac{\tau_A}{\frac{1}{2}\rho U_o^2} = -\,2\,k\,b\left(\frac{u'}{U_o}\right)^2 \qquad (2)$$

Using the amplification factor $a(R)$, $\frac{u'}{U_o}$ can be related to its initial value, $\left(\frac{u'}{U_o}\right)_i$, just upstream of the amplification zone:

$$\frac{\tau_A}{\frac{1}{2}\rho U_o^2} = -\,2\,k\,b\left(\frac{u'}{U_o}\right)_i^2 [a(R)]^2 \qquad (3)$$

Equation (3) is still quite general, τ_A will, of course, vary across the boundary layer and its magnitude will also depend upon the oscillation frequencies and on the Reynolds number. However, only the maximum value which τ_A can reach at a certain Reynolds number is necessary for the present discussion, since an attempt was made to find the Reynolds number at which τ_A first becomes equal to τ_L. Consequently,

$$\left(\frac{\tau_A}{\frac{1}{2}\rho U_o^2}\right)_{max} = -\,2\left\{k\,b\left(\frac{u'}{U_o}\right)_i^2 [a(R)]^2\right\}_{max} \qquad (4)$$

as function of the Reynolds number R_x. Now, the distribution of τ_A across the boundary layer has a maximum close to the so-called "critical layer" which is usually near the wall. Hence, for the transition criterion τ_L shall be replaced, approximately, by its value at the wall. Thus, in terms of the usual laminar skin friction coefficient,

$$\frac{\tau_L}{\frac{1}{2}\rho U_o^2} \doteq c_{f_L}$$

and the ratio $\frac{\tau_{A\,max}}{\tau_L}$ becomes:

$$\frac{\tau_{A\,max}}{\tau_L} \doteq -\frac{2}{c_{f_L}} \left\{ k\, b \left(\frac{u'}{U_o} \right)_i^2 [a(R)]^2 \right\}_{max} \qquad (5)$$

R_2 is then determined by

$$-\frac{2}{c_{f_L}} \left\{ k\, b \left(\frac{u'}{U_o} \right)_i^2 [a(R)]^2 \right\}_{max} \doteq 1 \qquad (6)$$

Application to Flat Plate Flow

The results obtained by Schlichting (references 6 and 7) can now be used to evaluate equation (5) or (6) numerically. Equation (1)* gives $a(R)_{max}$. The correlation coefficient k has been computed by Schlichting (reference 7) at one point on the lower branch and one point on the upper branch of the instability limit curve. Comparing the results at these two points it appears that k_{max} differs but little and thus the variation of k with Reynolds number is apparently very small. Since c_{f_L} and especially $a(R_x)$ vary rapidly with R_x, it is sufficient to replace $k(R)$ in equations (5) and (6) by a constant value. The maximum value $k = -0.18$ found by Schlichting is thus used in equation (5). The same argument apparently holds for b; in the neighborhood of the critical layer, b is of the order 0.1. This value also agrees with measurements (reference 1). The skin friction coefficient for the Blasius layer is given by

$$c_{f_L} = 0.664\, R_x^{-\frac{1}{2}}$$

Thus equation (5) finally becomes:

---

*The use of Schlichting's amplification function in the present analysis is not strictly correct; the oscillations are, of course, no longer "small perturbations" in the sense of the linear theory if τ_A becomes of the order of τ_L. The error involved is, however, probably not very large and the order of magnitude of R_2, which is of main concern here, will be unaffected.

$$\frac{\tau_{A\ max}}{\tau_L} = 0.016 \left(\frac{u'}{U_o}\right)_i^2 \sqrt{R_x}\, e^{1.11\times10^{-5} R_x} \qquad (7)$$

Figure 12 gives $\frac{\tau_{A\ max}}{\tau_L}$ plotted against R_x for different values of the initial fluctuation level. In considering the magnitude of the initial disturbance, it should be kept in mind that $\left(\frac{u'}{U_o}\right)_i$ is the fluctuation level with the most dangerous, that is, most highly amplified, frequency. Thus $\left(\frac{u'}{U_o}\right)_i$ is only a fraction of the total fluctuation level in the laminar layer upstream of the amplification zone.

Two facts are evident from figure 12.

(1) The slopes of the curves $\frac{\tau_{A\ max}}{\tau_L}$ versus R_x are very large in the neighborhood of $\frac{\tau_{A\ max}}{\tau_L} \doteq 1$. Hence R_2 does not depend too much upon the exact value of $\frac{\tau_{A\ max}}{\tau_L}$ which is chosen to define transition.

(2) Quantity $R_2 \gg R_1$ even with considerable initial fluctuation levels. (For example, with $\left(\frac{u'}{U_o}\right)_i$ = 1 percent, $R_2 = 10\ R_1$.)

The next step would logically involve relating the quantities entering equation (5) to factors known to influence transition. Especially the relation between $\left(\frac{u'}{U_o}\right)_i$ and the free stream turbulence level is very important.

At the present time only a few general considerations can be given in this connection and the main effects classified. It is hoped to obtain more complete relations in the future.

(1) Effect of free-stream turbulence.- Turbulence of the

free stream will affect the quantity $\left(\frac{u'}{U_o}\right)_i$ only. The effect will depend upon the free stream level $\left(\frac{u'}{U_o}\right)_f$ and upon the frequency distribution or upon the scale of turbulence. The relation between $\left(\frac{u'}{U_o}\right)_i$ and $\left(\frac{u'}{U_o}\right)_f$ is not simple and requires further study.

(2) Effect of pressure gradient.- The pressure gradient will affect at least two quantities in equation (3): namely, c_{f_L} and the amplification function $a(R)$. An adverse, that is, positive gradient causes a more rapid decrease of c_{f_L} with Reynolds number to $c_{f_L} = 0$ at separation, and as Schubauer and Skramstadt (reference 2) found, a larger amplification $a(R)$.

(3) Effect of roughness.- Small roughness elements, like free stream turbulence, will mainly affect $\left(\frac{u'}{U_o}\right)_i$. The value of $\left(\frac{u'}{U_o}\right)_i$ corresponding to a given roughness element will depend upon the element's height and also upon the width, since the latter influences the frequency distribution of the disturbance caused by the presence of the element.

CONCLUDING REMARKS

The results of measurements of boundary layer transition on the concave side of a plate with a 2.5-foot radius of curvature confirm the previous result that the mechanism leading to the breakdown of laminar flow differs essentially at convex and concave boundaries. Transition on convexly curved surfaces is due to the two-dimensional Tollmien-Schlichting type of instability as is the case with a flat plate. Transition on concave boundaries appears to result from the three-dimensional Görtler type of instability, and is thus related to the instability occurring in the flow between rotating cylinders.

No influence of pressure gradient on transition on the concave wall was found. The influence of a positive pressure-gradient on transition on convex boundaries is most pronounced in the neighborhood of zero pressure gradient. Free-stream turbulence appears to have about the same effect on the position of the transition point in concave and convex boundary layer flow.

The mean velocity profiles in the boundary layer of a concave plate with an effective radius of curvature around 10^{-3} was found to be very close to the Blasius flat-plate distribution.

A discussion of the breakdown mechanism of laminar flow shows the difference between the Reynolds number R_1 corresponding to the beginning of instability, in the sense of a small perturbation theory, and the Reynolds number R_2 corresponding to transition. The former number is well defined and can be predicted for a given case with good accuracy. The latter can be defined by the condition that at R_2 the maximum apparent shear due to the laminar boundary layer oscillations becomes equal to the laminar shearing stress at the wall for the undisturbed mean motion. A rough estimate of R_2 for the case of flat plate flow shows that even with considerable initial disturbances R_2 is much larger than R_1.

California Institute of Technology,
Pasadena, Calif., October 28, 1944.

REFERENCES

1. Liepmann, Hans W.: Investigations on Laminar Boundary-Layer Stability and Transition on Curved Boundaries. NACA ACR No. 3H30, 1943.

2. Schubauer, G. B., and Skramstad, H. K.: Laminar-Boundary-Layer Oscillations and Transition on a Flat Plate. NACA ACR, April 1943.

3. Görtler, H.: Über eine dreidimensionale Instabilität laminarer Grenzschichten an concaven Wänden. Nachrichten Gesellschaft der Wissenschaften zu Göttingen; neue Folge 2, No. 1.

4. Mock, W. C., Jr., and Dryden, H. L.: Improved Apparatus for the Measurement of Fluctuations of Air Speed in Turbulent Flow. NACA Rep. No. 448, 1932.

5. Goldstein, S.: Modern Developments in Fluid Dynamics. The Clarendon Press (Oxford), vol. I, 1938, p. 173.

6. Schlichting, H.: Zur Entstehung der Turbulenz bei der Plattenströmung. Nachrichten Gesellschaft der Wissenschaften zu Göttingen, Mathematisch-Physikalische Klasse, 1933, pp. 181-208.

7. Schlichting, H.: Amplitudenverteilung und Energiebilanz der kleinen Störungen bei der Plattenströmung. Nachrichten Gesellschaft der Wissenschaften zu Göttingen, Mathematisch-Physikalische Klasse, vol. 1, 1935, pp. 47-78.

8. Taylor, G. I.: Fifth International Congress for Applied Mechanics, 1938, pp. 294-310.

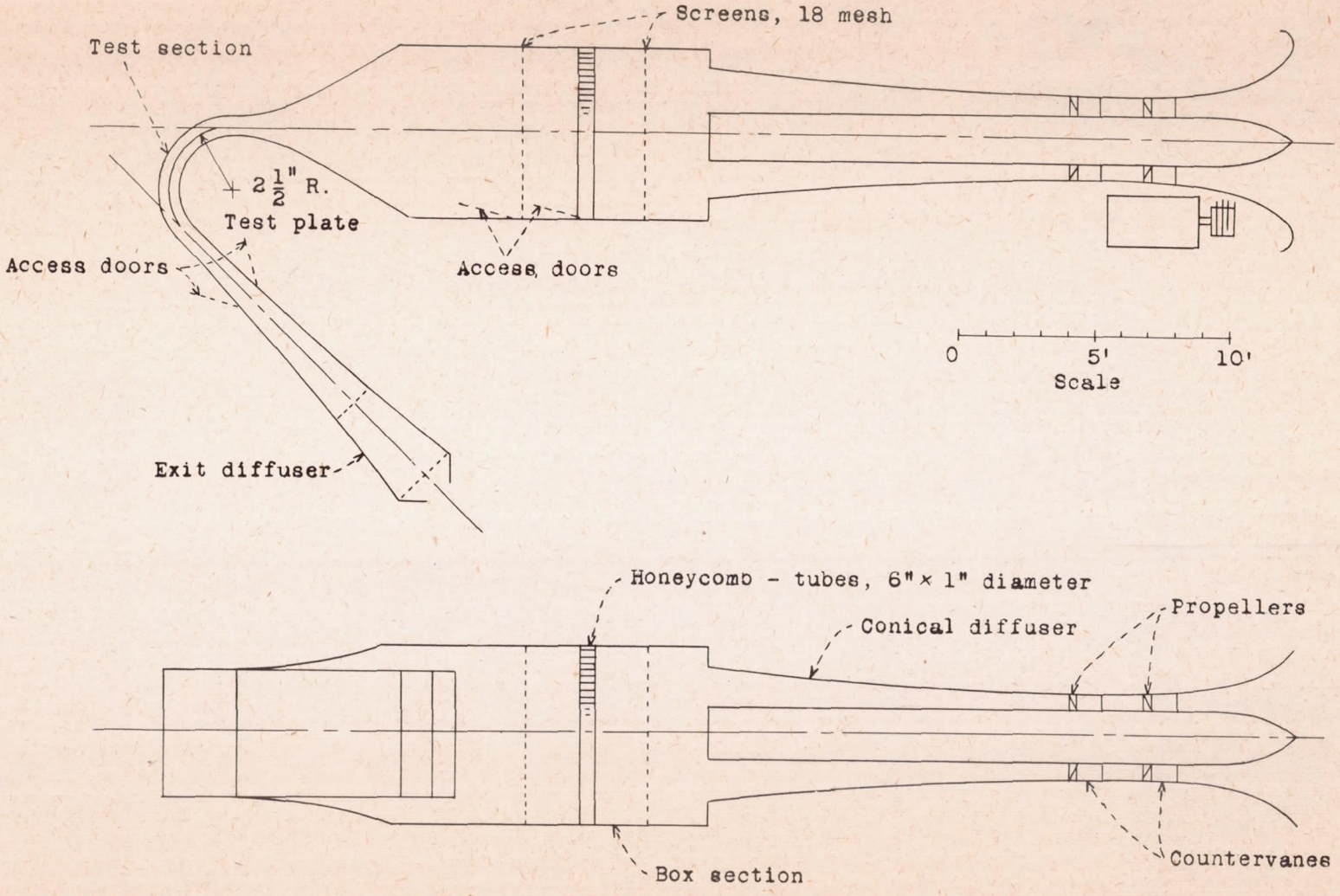

Figure 1.- Flow diagram of the boundary layer research tunnel.

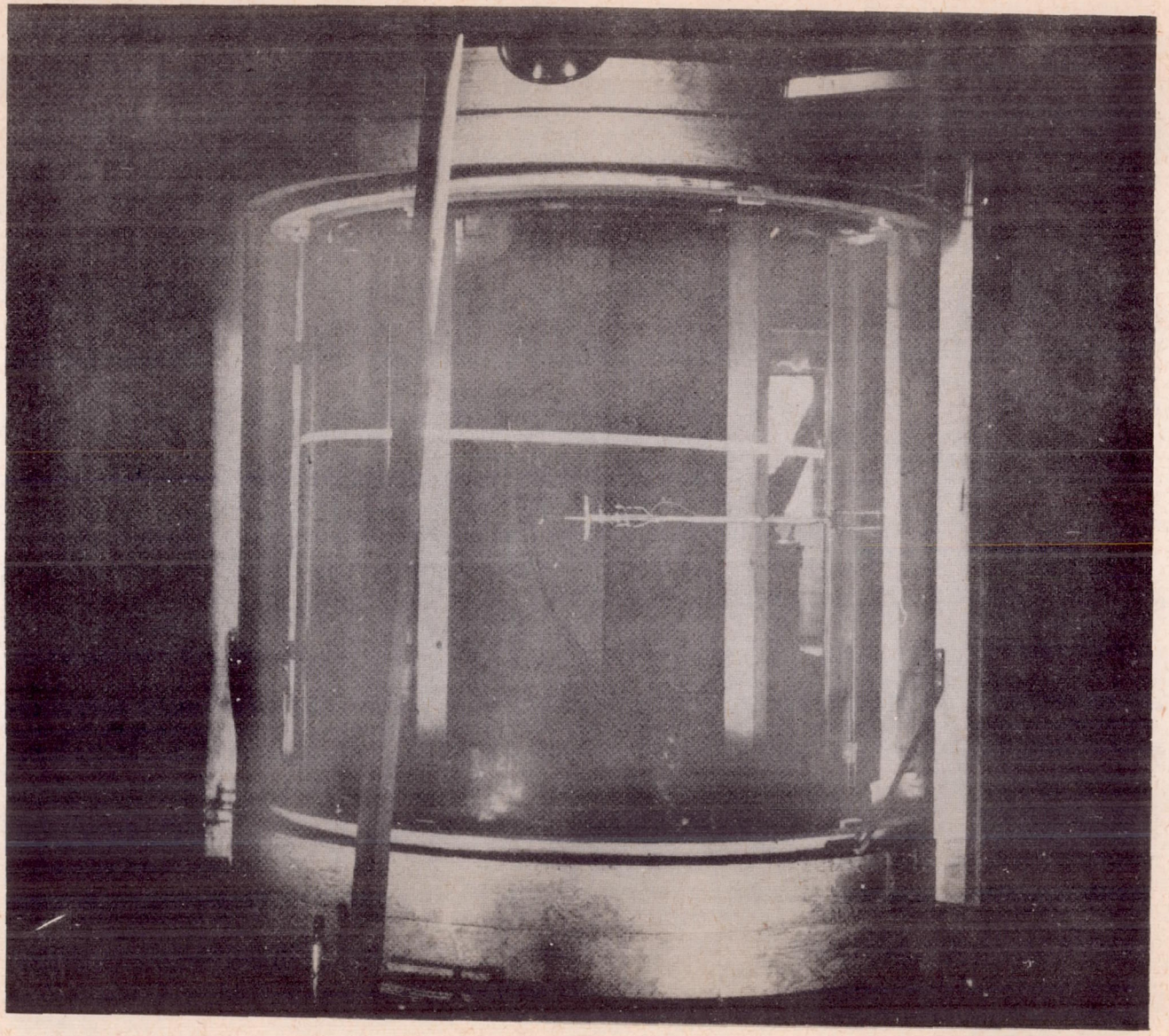

Figure 2.- Test plate with 2.5 foot radius of curvature.

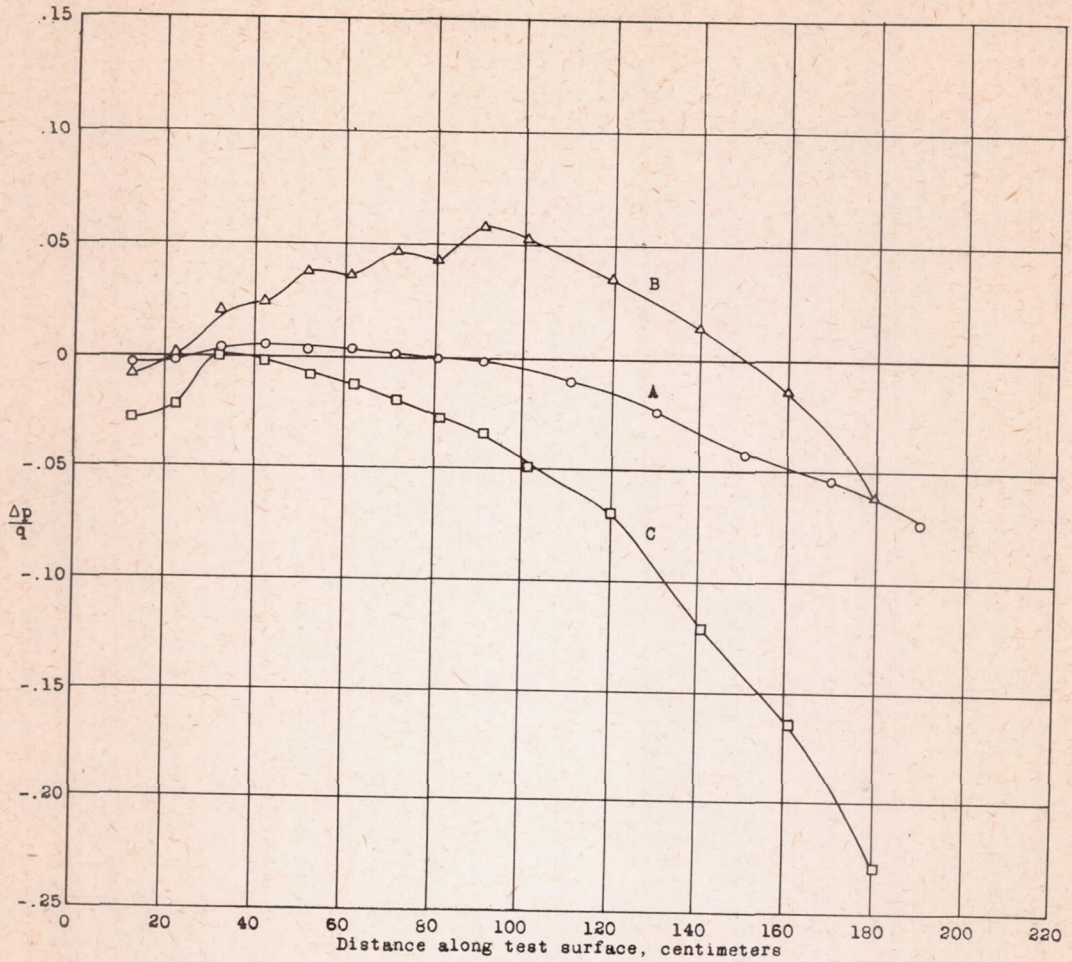

Figure 3.- Pressure gradients along the concave side of the plate with 2.5-foot radius of curvature for which transition was investigated.

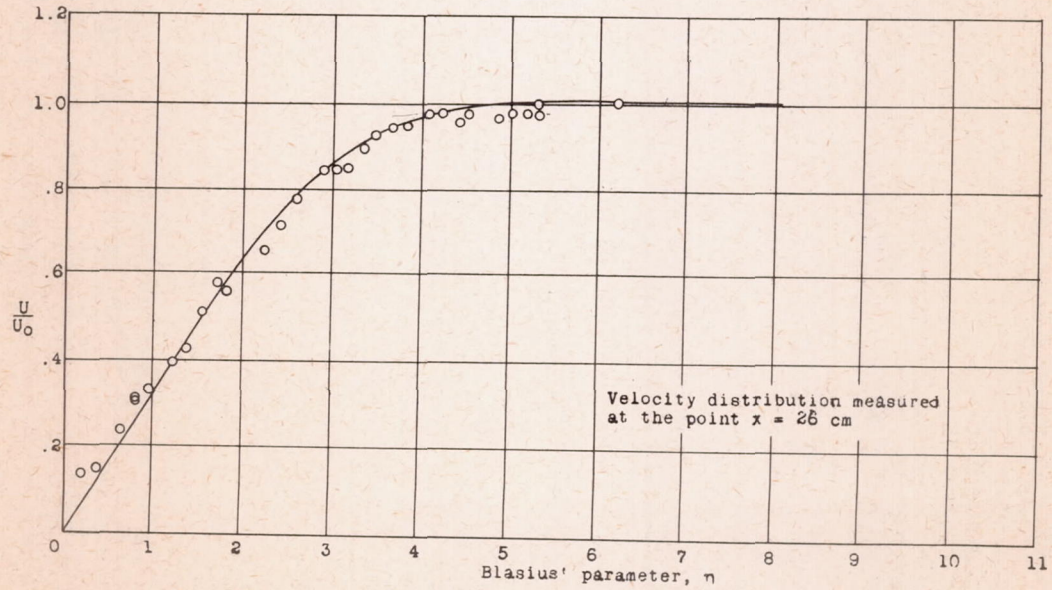

Figure 4.- Velocity distribution in the laminar boundary layer on the concave side of the plate with 2.5-foot radius of curvature as compared with Blasius' flat-plate solution.

W-87

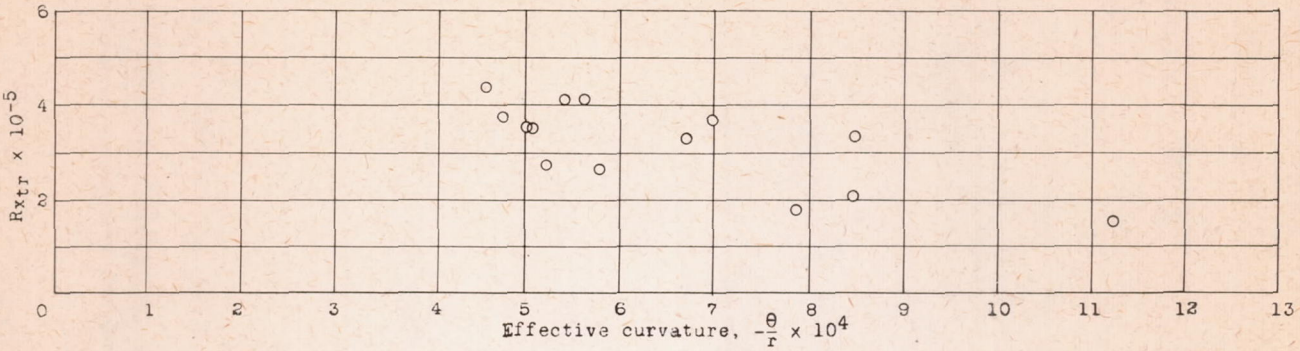

Figure 5.- Reynolds number of transition against the effective curvature on the concave side of the plate with 2.5-foot radius of curvature.

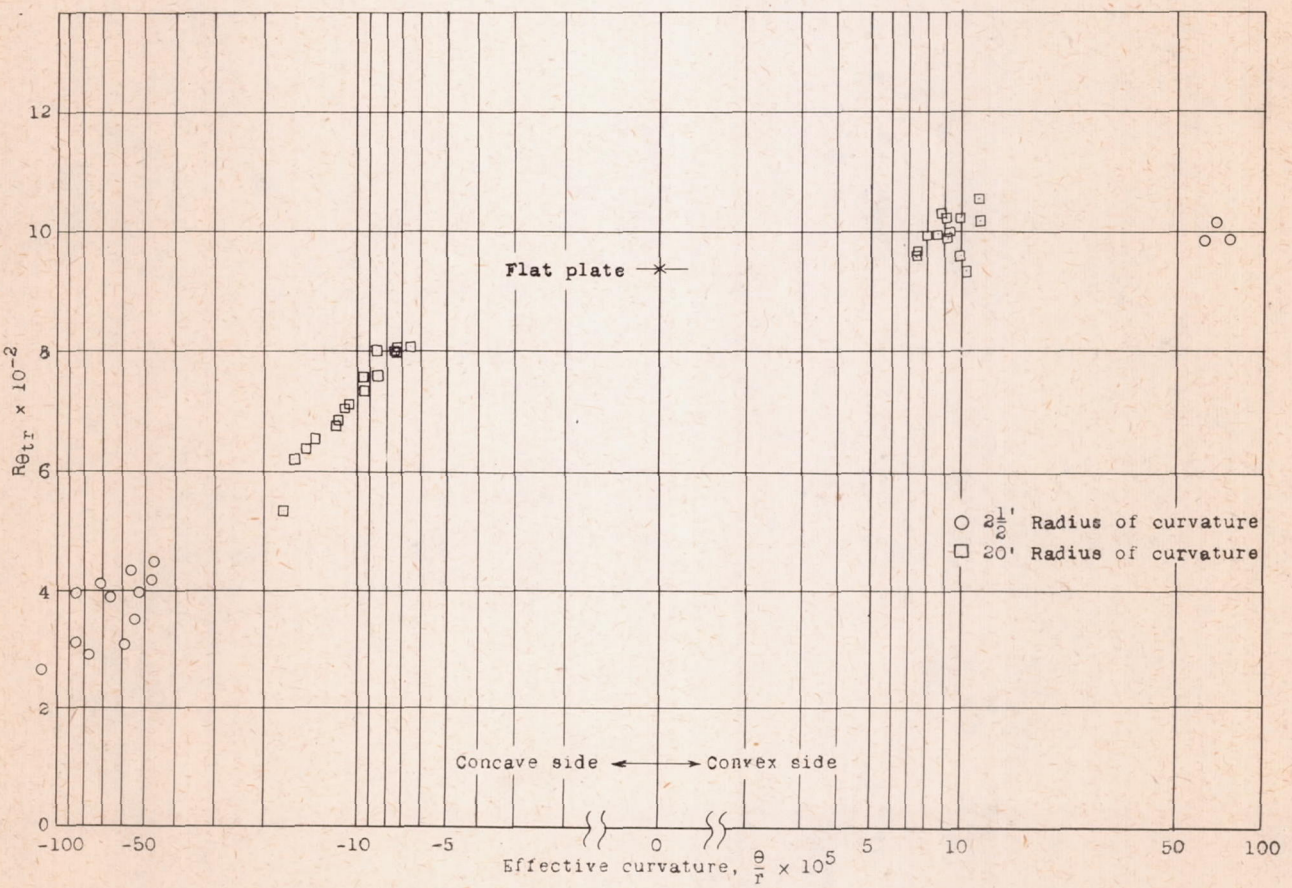

Figure 6.- Effect of curvature on transition. The arrows point to the value of $R_{\theta_{tr}}$ found for the flat plate.

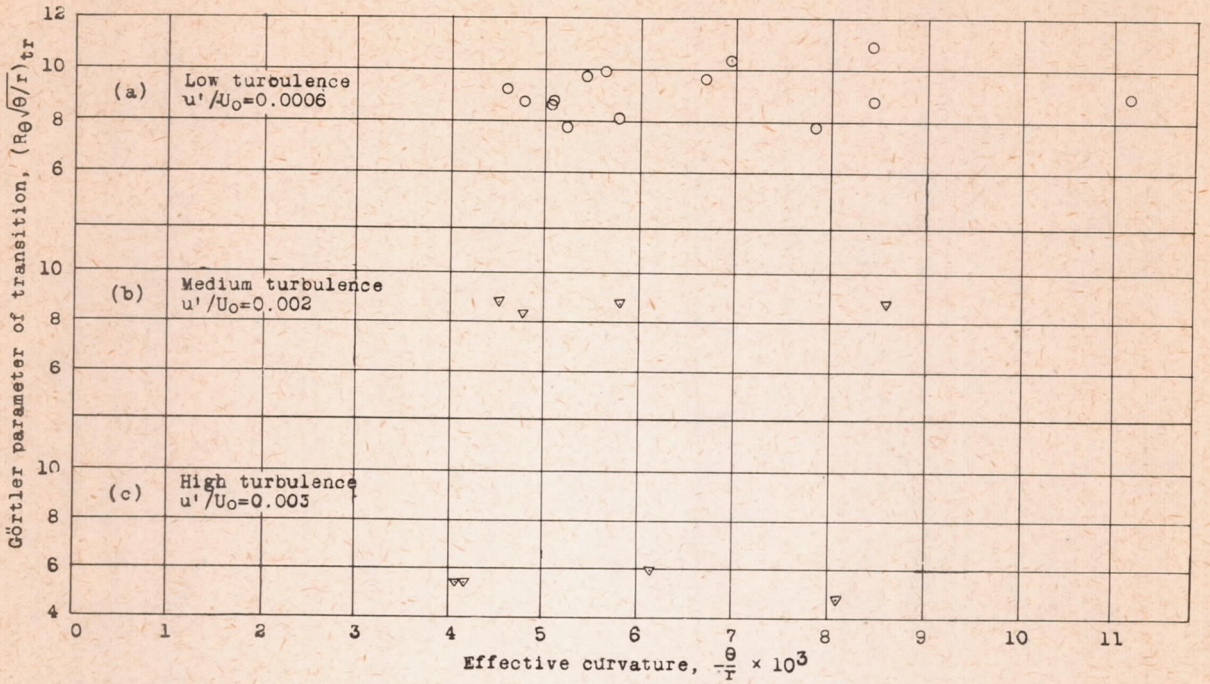

Figure 7.- Transition measurements on the concave side of the plate with 2.5-foot radius of curvature at three different turbulence levels of the free stream.

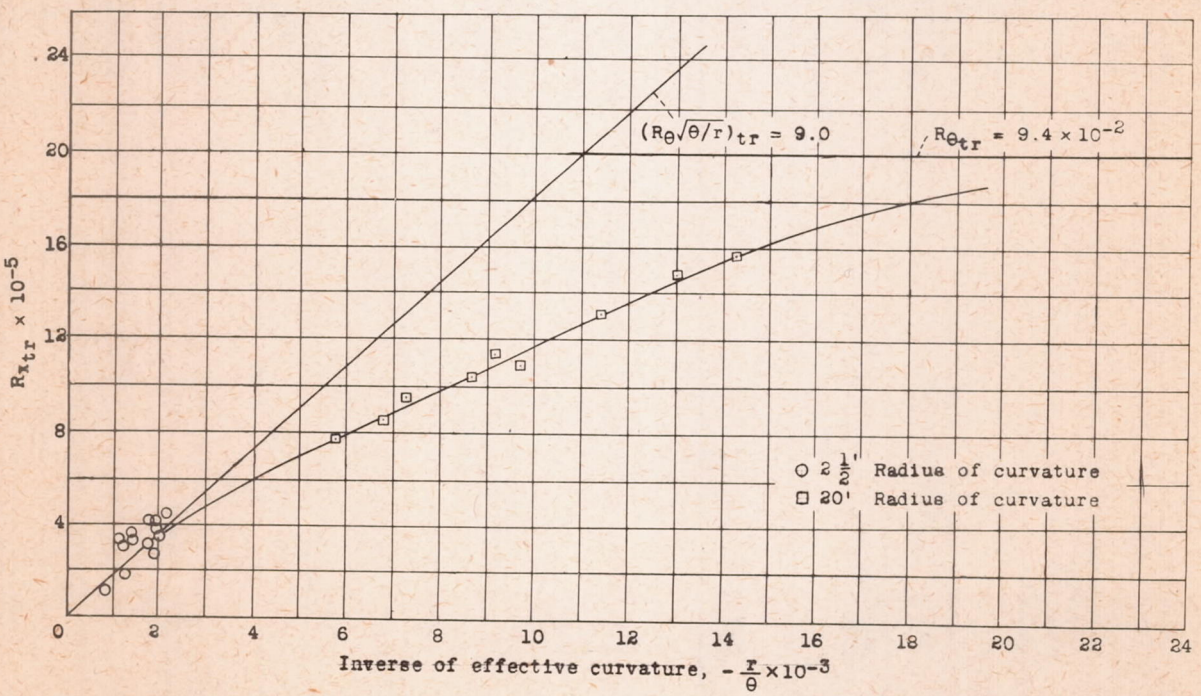

Figure 8.- Transition measurements on the concave sides of the plates of 2.5 and 20-foot radius of curvature.

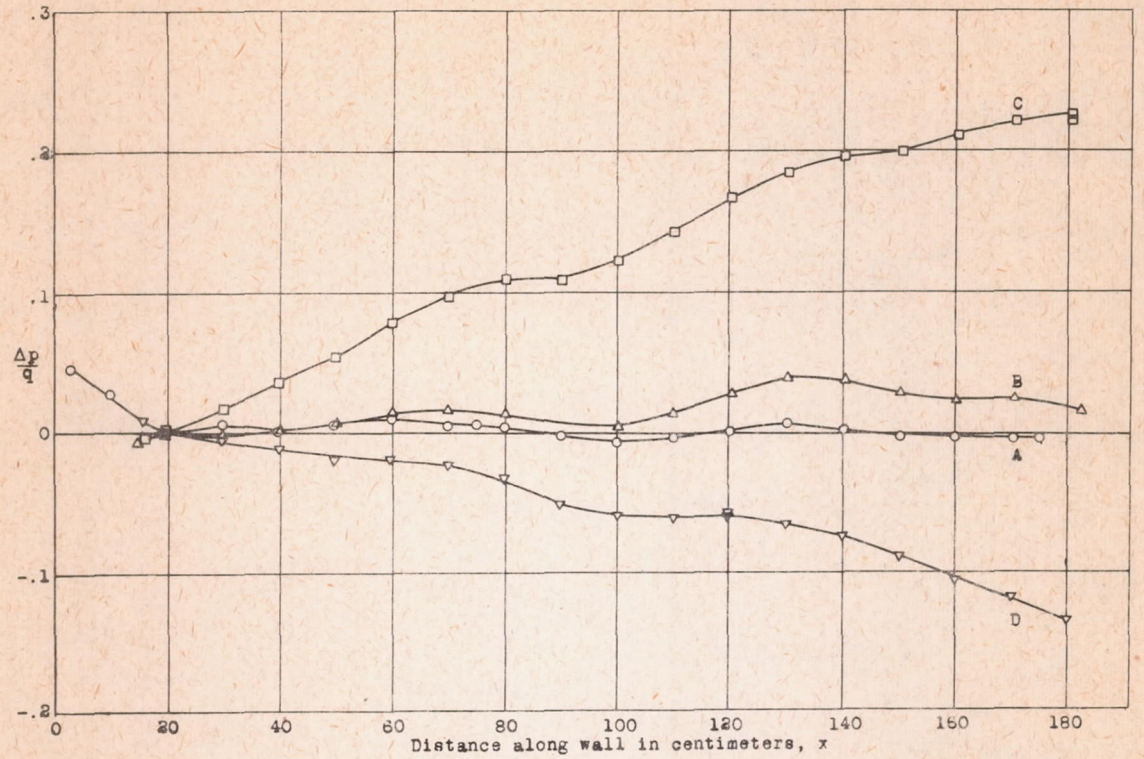

Figure 9.- Pressure gradients on the convex side of the plate of 20-foot radius for which transition was investigated.

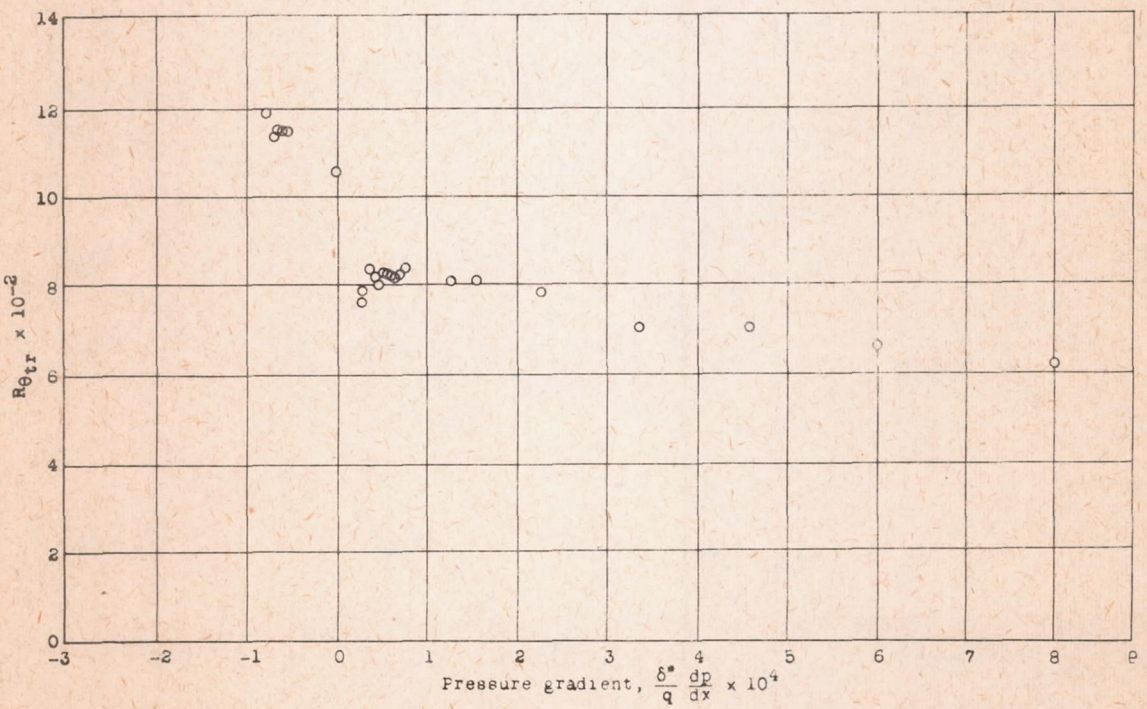

Figure 10.- Effect of the pressure gradient on transition for flow past the convex side of the plate with 20-foot radius of curvature.

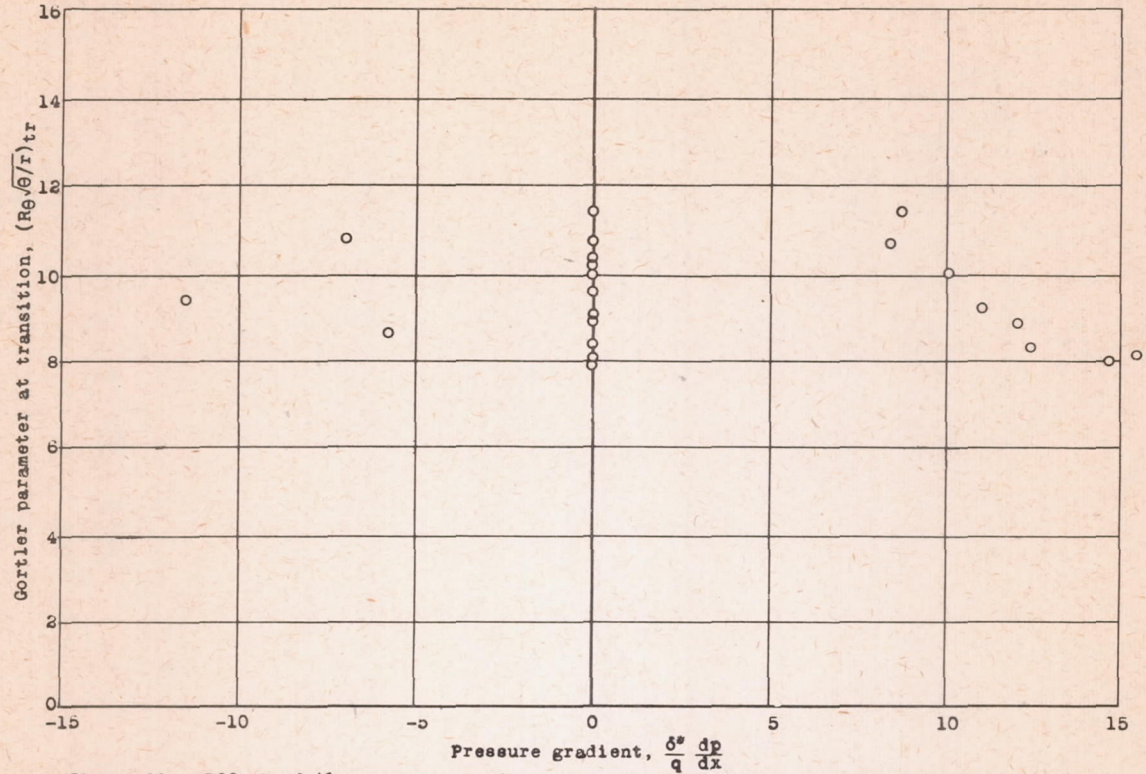

Figure 11.- Effect of the pressure gradient on transition on the concave side of the plate with 2.5-foot radius of curvature.

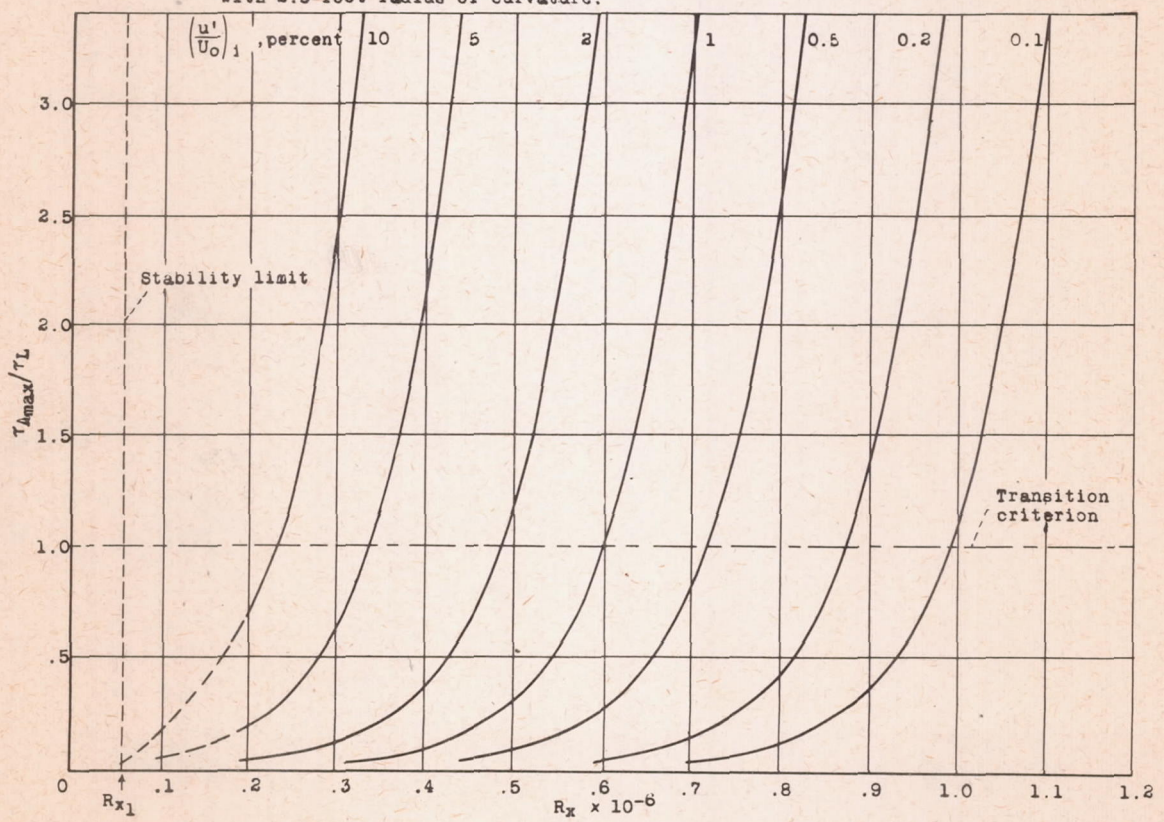

Figure 12.- Transition criterion for flow along a flat plate with different intensities of the initial disturbance.